Idelalisib inhibits experimental proliferative vitroretinopathy

Lijun Dong[1#], Haote Han[2, 3,4#], Xionggao Huang[5#], Gaoen Ma[6], Dong Fang[1], Hui Qi[1], Zhuo Han[2], Luping Wang[2], Jingkui Tian[2], Bart Vanhaesebroeck[7], Guoming Zhang[1], Shaochong Zhang[1*] and Hetian Lei[1*]

[1]Shenzhen Eye Hospital, Jinan University, Shenzhen Eye Institute, Shenzhen, China

[2]Institute of Cancer and Basic Medicine, Chinese Academy of Sciences, Cancer Hospital of the University of Chinese Academy of Sciences, Zhejiang Cancer Hospital, Hangzhou, China.

[3]Schepens Eye Research Institute of Massachusetts Eye and Ear, Boston, MA. USA

[4]Department of Ophthalmology, Harvard Medical School, Boston, MA, USA

[5]Department of Ophthalmology, the First Affiliated Hospital of Hainan Medical University, Haikou, China

[6]Department of Ophthalmology, the third Hospital of Xinxiang Medical University, Xinxiang, China

[7]Cancer Institute, University College London, London, UK

# These authors made equal contributions to this work

***Correspondence:** 18 Zetian Road, Futian District, Shenzhen, 518040, China. Email address: SZ: zhangshaochong@gzzoc.com, HL: leihetian18@hotmail.com

Abstract

Proliferative vitreoretinopathy (PVR) is a fibrotic eye disease that develops after rhegmatogenous retinal detachment surgery and open-globe traumatic injury. Idelalisib is a specific inhibitor of phosphoinositide 3-kinase (PI3K) δ. While PI3Kδ is primarily expressed in leukocytes, its expression is also considerably high in retinal pigment epithelial (RPE) cells, which play a crucial part in the PVR pathogenesis. Herein we show that GeoMx Digital Spatial Profiling uncovered strong expression of fibronectin in RPE cells within epiretinal membranes from patients with PVR, and that idelalisib (10 μM) inhibited Akt activation, fibronectin expression and collagen gel contraction induced by transforming growth factor (TGF)-β2 in human RPE cells. Furthermore, we discovered that idelalisib at a vitreal concentration of 10 μM, a non-toxic dose to the retina, prevented experimental PVR induced by intravitreally injected RPE cells in rabbits assessed by experienced ophthalmologists using an indirect ophthalmoscope plus a +30 D fundus lens, electroretinography, optical coherence tomography and histological analysis. These data suggested idelalisib could be harnessed for preventing patients from PVR.

Keywords: Idelalisib, PI3Kδ, TGF-β2, Akt, fibronectin, contraction, RPE, PVR

Introduction

Proliferative vitreoretinopathy (PVR) develops after rhegmatogenous retinal detachment (RRD) surgery and open-globe traumatic injury and is responsible for 5%–10% of all retinal detachment (1-5). The main feature of PVR is the formation of epi- or sub retinal membranes (ERMs) consisting of extracellular matrix and a variety of cells that include retinal pigment epithelial (RPE) cells, Muller's glia cells, fibroblasts, and macrophages (1,4,6). Among these cell types RPE cells are the crucial player in the pathogenesis of PVR (1,4,7). When the retina is detached or tears, some retinal cells (e.g. RPE cells) are activated by numerous factors such as growth factors, cytokines to undergo a variety of changes including synthesis of proteins (e.g., collagen, fibronectin), cell proliferation, epithelial mesenchymal transition (EMT), as well as cell migration. Consequently ERMs form and their contraction leads to retinal detachment (4,6,8-12).

Phosphoinositide (PI) 3-kinases (PI3Ks) play a critical part (13,14) in the pathogenesis of PVR. PI3Ks activated by receptor tyrosine kinases, G-protein coupled receptors or other factors can phosphorylate the 3-hydroxyl group of the PI's inositol ring. The resulting phosphorylation provides a docking site for a variety of signaling enzymes with PH (Pleckstrin Homology) domains including the serine/threonine protein kinase B (PKB, Akt). Akt plays a crucial role in cell survival and cell growth (15,16). In the family of PI3K there are eight isoforms classified into three classes (I, II and III) (15,16). PI3Kα, -β and -δ consisting of a regulatory p85 subunit and a catalytic subunit (p110α, -β and -δ, respectively) belong to the PI3K class IA, and they are regulated by the cell surface receptors including receptor tyrosine kinases (16,17). Noticeably, while PI3Kδ is primarily expressed in leukocytes (18), its expression is considerably high in RPE cells, and it is essential for vitreous-induced

Akt activation as well as proliferation, migration and contraction of RPE cells (2,19).

Idelalisib is a small molecule, which is a competitive inhibitor of the ATP binding site of p110δ (20,21). It has clinically been used for treating certain cancers (e.g., chronic lymphocytic leukemia) (21-24) and blocks vitreous-induced Akt activation and proliferation of RPE cells (2). Currently there is no approved medicine for preventing PVR even though huge efforts have been made on developing such drugs (6,10-12,25-29). Surgery to restore the retinal position is still the only option for treating PVR (27,30,31), but the visual outcome of the operation is poor as repeated detachment after surgery causes the retinal damage (26). Therefore, development of a pharmacological approach is urgent for preventing PVR.

We herein showed that idelalisib selectively inhibited transforming growth factor (TGF) -β2 -stimulated Akt activation, fibronectin expression and collagen gel contraction in human RPE cells and prevented experimental PVR in rabbits induced by intravitreally injected RPE cells, indicative of idelalisib as a promising medicine for treating PVR.

Materials and methods

Major reagents

Primary antibodies against p-Akt, Akt, and fibronectin were purchased from Cell Signaling Technology (Danvers, MA), and the antibody against β-Actin was from Santa Cruz Biotechnology (Santa Cruz, CA). Horseradish peroxidase-conjugated secondary antibodies of mouse anti-rabbit IgG, and goat anti-mouse IgG were purchased from Santa Cruz Biotechnology. Enhanced chemiluminescent substrate to detect horseradish peroxidase was ordered from Thermo Scientific (Waltham, MA).

Idelalisib was purchased from APExBIO (Houston, TX).

ARPE-19 cells are human RPE cells that were purchased from American Type Culture Collection (Manassas, VA), and RPEM cells were RPE cells derived from an ERM of a patient with grade C PVR as described previously (2,32). Both were cultured in Dulbecco's modified Eagle's medium/nutrient mixture (DMEM/F12, Gibco, Grand Island, NY) supplemented with 10% fetal bovine serum (FBS).

GeoMx Digital Spatial Profiling

GeoMx Immune Cell Profiling Panel Human Protein Core for nCounter kit, GeoMx Hyb Code Pack Protein kit, GeoMx Nuclear Stain Morphology Kit, GeoMx Protein Slide Prep Kit, GeoMx Hyb Buffer, GeoMx DSP Collection Plates 96, GeoMx DSP Instrument Buffer Kit and nCounter Master Kit were purchased from Nanostring (Nanostring Technologies, WA).

This experiment was performed as described previously [33,34]. Briefly, formalin-fixed OCT-embedded ERM and normal breast epithelial tissue slides were washed thrice for 5 minutes, and the slides with the samples in 1 x citric acid buffer were transferred into a pressure cooker to be steamed for 15 minutes. Subsequently, the slides were cooled down at room temperature naturally within 30-60 minutes, and then washed once in Tris-based solution with 0.01% triton (TBST). The slides were then stained with fluorescently labeled morphology markers (CD45, Pan-cytokeratin) for 1 hour and then washed twice in TBST. Finally, an antibody mix (GeoMx Immune Cell Profiling Panel) was added to slides and incubated at 4°C overnight. SYTO staining (GeoMx Nuclear Stain Morphology Kit) was used for staining nuclei. Slides were loaded on the GeoMx microscope for imaging and barcode acquisition, following the manufacturer supplied protocol. ROIs were segmented into

PanCK-positive and CD45-positive areas of interest.). ROI into 96-well plate (GeoMx DSP Collection Plates) was collected and transferred to n-counter to read. The data were analyzed by a DSP machine.

Western blot

Western blot was conducted as described in previous reports (2,13,35-37). Briefly, when cells were grown to 90% confluence in 24-well plates, they were serum starved for 24 hours, and then treated with TGF-β2 (10 ng/ml, R& D systems, Minneapolis, MN) in the presence or absence of idelalisib (10 μM) for additional 48 hours. Proteins from treated cells were extracted in an extraction buffer and separated by 10% SDS-polyacrylamide gel electrophoresis. The proteins in the gel were then transferred to polyvinylidene difluoride membranes for analysis using desired antibodies (2,35,38-40).

Collagen gel contraction assay

This assay was conducted as described in previous reports (2,13,35-37). Briefly, when cells grew to 90% confluence, they were collected and re-suspended at a density of 1×10^6 in 1.5 mg/ml of neutralized PureCol type I bovine collagen solution (Advanced BioMatrix, San Diego, CA) (pH 7.2) on ice. The mixture of the cells with the collagen was then transferred into 24-well tissue culture plates (300 μl/well). After incubated at 37°C for 90 minutes, 0.5 ml DMEM/F12 or in DMEM/F12 with 10 ng/ml TGF-β2 plus or minus idelalisib (10 μM) was added on the top of polymerized collagen gel in the 24-well plate, which was then photographed on day 3. The gel diameter was then measured, and the gel area was calculated using the formula $3.14 \times r^2$ for further statistic analyses.

Experimental PVR in rabbits

As previously described (6,35,36,41,42), PVR was induced in the right eyes of 8-weeks-old Dutch Belted rabbits (Covance, Denver, PA). Briefly, a gas vitrectomy was performed by injecting 0.1 ml of perfluoropropane (C3F8) (Alcon, Fort Worth, TX) into the vitreous cavity 4 mm posterior to the corneal limbus. One week later, all 20 rabbits were injected with platelet-rich plasma (0.1 ml) and 3.0 x 10^5 cells of RPEM cells with idelalisib (final 10 μM) or its vehicle DMSO (final 0.01%) under an operative microscope. The retinal status was examined with an indirect ophthalmoscope plus a +30 D fundus lens on days 1, 3, 5, 7, 14, 21 and 28 by two masked ophthalmologists. PVR was graded according to the Fastenberg classification from 0 through 5 (35,42,43).

On day 28, 4 representative rabbits from stages 1 and 5 were in the dark for one hour. The rabbits were deeply anesthetized with intramuscular anesthesia consisting of ketamine (30-50 mg/kg), xylazine (5-10 mg/kg) and acepromazine (1 mg/kg). Depth of anesthesia was verified by the absence of the toe pinch withdrawal reflex. The pupils were dilated with topical 1% tropicamide to view the fundus. Electroretinogram (ERG) analysis was performed as previously described [35]. Following ERG, optical coherence tomography (OCT) was taken using spectral domain (SD)-OCT system (Bioptigen Inc., Durham, NC). The animals were then sacrificed, the eyes were enucleated, and representative eyeballs were fixed with 10% formalin for histology analysis. This animal experiment was conducted at the animal facility of the Schepens Eye Research Institute (Boston, MA).

The protocol for the use of animals was approved by the Schepens Eye Research Institute Animal Care and Use Committee (Boston, MA), and all animal surgeries

adhered to the ARVO Statement for the Use of Animals in Ophthalmic and Vision Research.

Statistics

Data were analyzed as described previously (2,44). Briefly, data from at least three independent experiments were analyzed using ordinary one-way ANOVA followed by the Tukey honest significant difference (HSD) post hoc-test. Animal experimental data were analyzed using a Mann Whitney test (6,35,36,42). p less than 0.05 was considered a significant difference.

Results

Fibronectin is upregulated in the RPE cells within ERMs from patients with PVR

The GeoMx Digital Spatial Profiling (DSP) integrates with current histology methods to have quickly, robust and reproducible spatial omics data[34]. To better understand the PVR pathogenesis, we used GeoMx DSP to analyze the protein expression of different tissues and cell types in ERMs from patients with PVR. The results showed that in comparison of the normal control tissue CD68 and fibronectin were significantly up-regulated in the ERMs (Fig. 1A, B). Notably, CD45 is a marker of all hematopoietic cells, whereas CD68 is indicative of macrophage activation and able to promote NF-κB nuclear translocation and inflammation, indicating that there is infiltration of activated immune cells in the ERMs from patients with PVR.

DSP also showed that in comparison of CD45-positive cells in the RPE cells within the ERMs, fibronectin, α-smooth muscle actin, and pan-cytokeratin were

significantly up-regulated, but CTLA-4 (cytotoxic T-lymphocyte-associated protein 4 or CD152) and PD-L1 (programmed death-ligand 1) functioning as immune checkpoints and down-regulate immune responses were down-regulated (Fig. 1A, C).

The heatmap and PCA analysis indicated that there was significant difference in cells related to cell migration and inflammation between the ERMs and control tissues (Fig. 1D, E, F and G). In agreement with previous studies (4,8,40,45,46), these DSP results further demonstrate that inflammation and EMT play an important role in the pathogenesis of PVR.

Idelalisib inhibits TGF-β2-induced Akt activation and fibronectin expression

Levels of TGF-β2 in the vitreous are elevated in eyes with intraocular fibrosis including PVR (47), and PI3Kδ plays an essential role in vitreous-induced Akt activation and cellular responses intrinsic to PVR (2,19). In addition, TGF-β2 is a prominent cytokine to induce expression of fibronectin, one of the protein markers for EMT playing an important role in the development of PVR (12,47). While the receptor serine/threonine kinases activated by TGF-β2 operate mainly through the Smad (e.g., phosphorylating Smad2) to regulate gene expression, they can also stimulate the PI3K-Akt signaling pathway. Thereby we hypothesized that inhibition of PI3Kδ with its specific inhibitor idelalisib was able to prevent TGF-β2-induced fibronectin expression and Akt activation in RPE cells. As shown in Fig. 2, western blot analysis showed that TGF-β2 treatment for 48 hours indeed induced Akt activation (5.1 ± 0.6 fold) as well as fibronectin expression (7.8 ± 0.8 fold) in human RPE cells (ARPE-19), and that idelalisib abrogated these actions induced by TGF-β2 in human RPE cells.

Idelalisib suppresses TGF-β2 -induced collagen gel contraction

In the PVR pathogenesis, the contraction of the ERMs eventually causes retinal detachment (7,48,49). To mimic this process, an *in vitro* assay of collagen gel contraction has been developed (2,35,42). This assay can be employed for evaluation of a drug's potential capabilities of inhibiting PVR *in vitro*. To examine if idelalisib could inhibit TGF-β2-induced cell contraction, RPEM cells derived from an ERM from a patient with PVR were mixed with collagen solution to form a collagen gel, and media on the top of this collagen gel were treated with TGF-β2 in the presence or absence of idelalisib. The results showed (Fig. 3) that while TGF-β2 treatment for 48 hours stimulated the contraction of the mixture of collagen with RPEM cells from 168.5 ± 8.1 mm^2 to 78.0 ± 12.8 mm^2, idelalisib significantly blocked this TGF-β2-induced cellular event, that is, the collagen gel area was 131.2 ± 5.9 mm^2. These results indicate that idelalisib has high potential to inhibiting PVR *in vivo*.

Idelalisib prevents experimental PVR in rabbits

As inactivation of PI3Kδ attenuated PVR-related signaling events (e.g., Akt activation) and cellular responses (e.g., collagen gel contraction) induced by vitreous (2,19) and TGF-β2 (Figs. 2-3), we next sought to clarify whether inhibition of PI3Kδ could prevent experimental PVR. The animal model of experimental PVR that most researchers use is to intravitreally inject cells into the rabbit eyes because the lens of rabbits is relatively small and this advantage can maximally limit the changes to the lens and retina when performing intravitreal injections. In this experimental model of PVR the rabbits are examined for the formation of cellular membranes in the vitreous because their contraction can lead to retinal detachment (6,35,36,41,42,50).

We firstly evaluated the toxicity of idelalisib to the rabbit retina. We identified the minimum effective dose (1 μM) and maximum 20 μM) tolerated dose of idelalisib to RPE cells derived from patients with PVR (defined as RPEM cells) (2), and we sought to establish the maximum dose of idelalisib that could be injected into the vitreous without overt retinal toxicity. We chose RPEM cells for these studies because they were most relevant to human PVR.

To this end, we intravitreally injected a total of 0.1 ml idelalisib to achieve a final vitreal concentration of 10 or 20 μM after a gas vitrectomy in 6 rabbits. Examination of rabbit eyes with an indirect ophthalmoscope plus a +30 D fundus lens on days 1, 3, 5, 7 by two ophthalmologists did not reveal any toxicity to the injected eyes. To confirm this observation, on day 7 electroretinography (ERG) was harnessed to monitor the retinal function. As shown in Fig. 4A, in comparison with the left un-injected eyes, there were no obvious changes in the a-waves and b-waves in the idelalisib-injected eyes. Examination with optical coherence tomography (OCT) also showed that there were not significant changes in retinal thickness, indicating that these two doses (10 and 20 μM) of idelalisib to rabbit retinas were well-tolerated (Fig. 4B). In addition, histological analysis further demonstrated that there was no significant change in the retinal structure after intravitreal injection of idelalisib into the right eyes in comparison with the un-injected left eyes (Fig. 4C). Furthermore, our previous experimental results also demonstrated that idelalisib at 10 μM did not cause obvious adverse effects in mouse eyes examined by ERG, OCT and histological analysis of the retinas[51]. Consequently, we chose the 10 μM dose for the subsequent experiments.

To determine whether idelalisib could prevent PVR, after a gas vitrectomy we intravitreally injected platelet-rich plasma, RPEM cells, and then either idelalisib (10

μM) or its solvent DMSO (0.01%) as a negative control（35,42). As shown in Fig. 5A, on day 28 there were 7 injected eyes (87.5%) being retinal detachment（PVR stages 4-5） among the 8 control-injected rabbits, and there was only one injected eye (11.1%) being retinal detachment （PVR stage 3）among the 9 idelalisib-injected rabbits evaluated by two ophthalmologists with an indirect ophthalmoscope plus a +30 D fundus lens. These results indicated that severe PVR stages were significantly reduced in rabbits injected with idelalsib, but there were 7 (77.8%) among the 9 idelalisib-treated rabbits developing epi-retinal membranes (PVR stages 1-2) (Fig. 5A).

To confirm the PVR stages evaluated by the ophthalmologists with an indirect ophthalmoscope (Fig. 5A), the PVR status of 4 rabbits with stage 1 or 5 was further evaluated by ERG (Fig. 5B) indicating that 1) the injected right eyes with PVR did not affect the un-injected left ones, 2) minor vitreous fibrosis (PVR stage 1) did not significantly affect retinal function; and 3) the retinal detachment caused retinal dysfunction in the eye with PVR stage 5. OCT analysis of 6 eyes with 2 normal eyes as a control confirmed that 1) there were fibrotic tissues attaching the retina in the eye with PVR stage 2 (1 eye); 2) the fibrotic tissues attached the retina causing the retinal detachment in the eye with PVR stage 3 (1 eye); the retina got total detachment from its original position with PVR stage 5 (2 eyes) (Fig. 5C). Histological analysis further verified the fibrosis in PVR stages 2, 3 and 5 evaluated with an indirect ophthalmoscope and OCT (Fig. 5D). These studies demonstrate that idelalisib effectively protects rabbits from developing the severe stages (stages 4 and 5) of PVR, suggesting this pharmacological intervention could be further tested for protecting patients from developing PVR.

Discussion

In the present study, fibronectin was identified by the advanced technology of the GeoMx DSP to be strongly expressed in RPE cells within the ERMs from patients with PVR (Fig. 1). This result is consistent with previous findings[52-54]. Subsequently, we discovered that idelalisib inhibited TGF-β2-induced Akt activation, fibronectin expression and collagen gel contraction (Figs. 2-3), and these signaling events and cellular responses are related to PVR. PVR is still a major obstacle to successfully correct retinal detachment despite gradual improvements in surgical success rates over the past decades; in particular, there are over 75% of postsurgical re-detachments in developing PVR (55). However, there is still no effective medicine for this blinding disease. Thereby we evaluated the potential of the FDA approved medicine idelalisib for preventing PVR and found that this drug significantly inhibited experimental PVR in an intravitreal cell injection rabbit model (Figs. 4-5). In this animal experiment, we intravitreally injected RPE cells (3 x 10^6 cells /eye) derived from an ERM from a patient with PVR (32) into Dutch belted rabbits, leading to severe PVR with retinal detachment (Stages 3-5) in seven of 8 eyes by day 28 （Fig. 5）. Whereas other investigators reported that these RPEM cells induced less severe PVR in New Zealand albino rabbits, that is, by day 28 there was only one eye developed extensive tractional retinal detachment among the 24 experimental eyes injected with 1 x 106 cells/eye (32). The different results of these two experiments might be due to using different species of rabbits and cell numbers. In addition, in our current experiment, rabbits were of a younger age (8 weeks) than those we used previously (16-24 weeks), so the younger rabbits might be easier to develop severer PVR in this cell injection model based on our unpublished observation. In general, RPE cells have less potential

to induce experimental PVR in rabbits compared to fibroblasts based on our previous experimental results (6,35,36,39,41,42,56).

In order to develop therapeutic approaches to PVR, so far there are a lot of medical treatments tested including antineoplastic drugs (e.g., 5-fluorouracil, cisplatin 57, methotrexate58), tyrosine kinase inhibitors (e.g., dasatinib) (59), protein kinase C inhibitors (e.g., herbimycin A) (60), TGF-β receptor inhibitors (e.g., LY-364947) (61), p53 inhibitors (e.g., nutlin-3) (42), scavengers of reactive oxygen species (e.g., N-acetyl-cysteine) (35), and other drugs (55). In spite of these considerable efforts, clinical success is still unreached. Inactivation of PI3Kδ in mice failed to show any detectable phenotypes in their embryos and adult eyes, but its expression is enhanced in pathological conditions (51). Given the hardly detectable expression of PI3Kδ in mouse photoreceptor cells (51), it is likely that its activity in these cells is not essential. These findings indicate that PI3Kδ is a promising target for PVR therapy.

In this report, we demonstrate that idelalisib, an FDA approved specific inhibitor for PI3Kδ, inhibits experimental PVR in a rabbit model, uncovering the potential of this agent as a potential PVR prophylactic, addressing a currently unmet clinical need (62).

References

1 Jiang H, Luo J & Lei H. The roles of mouse double minute 2 (MDM2) oncoprotein in ocular diseases: A review. *Exp Eye Res*, 217, 108910(2022).

2 Xin T, Han H, Wu W, Huang X, Cui J, Matsubara JA, *et al.* Idelalisib inhibits vitreous-induced Akt activation and proliferation of retinal pigment epithelial

cells from epiretinal membranes. *Exp Eye Res* **190**, 107884(2020).

3 Zandi S, Pfister IB, Traine PG, Tappeiner C, Despont A, Rieben R, *et al.* Biomarkers for PVR in rhegmatogenous retinal detachment. *PloS one* **14**, e0214674(2019).

4 Schiff L, Boles NC, Fernandes M, Nachmani B, Gentile R, Blenkinsop TA. P38 inhibition reverses TGFbeta1 and TNFalpha-induced contraction in a model of proliferative vitreoretinopathy. *Commun Biol* **2**, 162, (2019).

5 Justin GA, Baker KM, Brooks DI, Ryan DS, Weichel ED, Colyer MH. Intraocular Foreign Body Trauma in Operation Iraqi Freedom and Operation Enduring Freedom: 2001 to 2011. *Ophthalmology* **125**, 1675-1682 (2018).

6 Zhou G, Duan Y, Ma G, Wu W, Hu Z, Chen N, *et al.* Introduction of the MDM2 T309G Mutation in Primary Human Retinal Epithelial Cells Enhances Experimental Proliferative Vitreoretinopathy. *Invest Ophthalmol Vis Sci* **58**, 5361-5367 (2017).

7 Pennock S, Haddock LJ, Eliott D, Mukai S & Kazlauskas A. Is neutralizing vitreal growth factors a viable strategy to prevent proliferative vitreoretinopathy? *Prog Retin Eye Res* **40**, 16-34 (2014).

8 Tamiya, S. & Kaplan, H. J. Role of epithelial-mesenchymal transition in proliferative vitreoretinopathy. *Exp Eye Res* **142**, 26-31(2016).

9 He H, Kuriyan AE, Su CW, Mahabole M, Zhang Y, Zhu YT, *et al.* Inhibition of Proliferation and Epithelial Mesenchymal Transition in Retinal Pigment Epithelial Cells by Heavy Chain-Hyaluronan/Pentraxin 3. *Sci Rep* **7**, 43736

(2017).

10 Wang ZY, Zhang Y, Chen J, Wu LD, Chen ML, Chen CM, *et al.* Artesunate inhibits the development of PVR by suppressing the TGF-beta/Smad signaling pathway. *Exp Eye Res* **213**, 108859 (2021).

11 Song Y, Liao M, Zhao X, Han H, Dong X, Wang X, *et al.* Vitreous M2 Macrophage-Derived Microparticles Promote RPE Cell Proliferation and Migration in Traumatic Proliferative Vitreoretinopathy. *Invest Ophthalmol Vis Sci* **62**, 26 (2021).

12 Yang S, Li H, Yao H, Zhang Y, Bao H, Wu L, *et al.* Long noncoding RNA ERLR mediates epithelial-mesenchymal transition of retinal pigment epithelial cells and promotes experimental proliferative vitreoretinopathy. *Cell Death Differ* **28**, 2351-2366(2021).

13 Lei H, Rheaume MA, Velez G, Mukai S & Kazlauskas A. Expression of PDGFR{alpha} Is a Determinant of the PVR Potential of ARPE19 Cells. *Invest Ophthalmol Vis Sci* **52**, 5016-5021(2011).

14 Ikuno Y, Leong FL & Kazlauskas A. PI3K and PLCgamma play a central role in experimental PVR. *Invest Ophthalmol Vis Sci* **43**, 483-489 (2002).

15 Vanhaesebroeck, B., Guillermet-Guibert, J., Graupera, M. & Bilanges, B. The emerging mechanisms of isoform-specific PI3K signalling. *Nature reviews. Molecular cell biology* **11**, 329-341 (2010).

16 Bilanges B, Posor Y & Vanhaesebroeck B. PI3K isoforms in cell signalling and vesicle trafficking. *Nature reviews. Molecular cell biology* **20**,

515-534(2019).

17 Whitehead, M. A., Bombardieri, M., Pitzalis, C. & Vanhaesebroeck, B. Isoform-selective induction of human p110delta PI3K expression by TNFalpha: identification of a new and inducible PIK3CD promoter. *Biochem J* **443**, 857-867(2012).

18 Vanhaesebroeck B, Welham MJ, Kotani K, Stein R, Warne PH, Zvelebil MJ, *et al.* P110delta, a novel phosphoinositide 3-kinase in leukocytes. *Proc Natl Acad Sci U S A* **94**, 4330-4335 (1997).

19 Han H, Chen N, Huang X, Liu B, Tian J, Lei H. Phosphoinositide 3-kinase delta inactivation prevents vitreous-induced activation of AKT/MDM2/p53 and migration of retinal pigment epithelial cells. *J Biol Chem* **294**, 15408-15417 (2019).

20 Gopal AK, Kahl BS, de Vos S, Wagner-Johnston ND, Schuster SJ, Jurczak WJ, *et al.* PI3Kdelta inhibition by idelalisib in patients with relapsed indolent lymphoma. *N Engl J Med* **370**, 1008-1018(2014).

21 Somoza JR, Koditek D, Villasenor AG, Novikov N, Wong MH, Liclican A, *et al.* Structural, biochemical, and biophysical characterization of idelalisib binding to phosphoinositide 3-kinase delta. *J Biol Chem* **290**, 8439-8446 (2015).

22 Brown JR, Byrd JC, Coutre SE, Benson DM, Flinn IW, Wagner-Johnston ND, *et al.* Idelalisib, an inhibitor of phosphatidylinositol 3-kinase p110delta, for relapsed/refractory chronic lymphocytic leukemia. *Blood* **123**, 3390-3397

(2014).

23 Flinn IW, Kahl BS, Leonard JP, Furman RR, Brown JR, Byrd JC, *et al.* Idelalisib, a selective inhibitor of phosphatidylinositol 3-kinase-delta, as therapy for previously treated indolent non-Hodgkin lymphoma. *Blood* **123**, 3406-3413 (2014).

24 Furman RR, Sharman JP, Coutre SE, Cheson BD, Pagel JM, Hillmen P, *et al.* Idelalisib and rituximab in relapsed chronic lymphocytic leukemia. *N Engl J Med* **370**, 997-1007 (2014).

25 Sadaka A & Giuliari GP. Proliferative vitreoretinopathy: current and emerging treatments. *Clin Ophthalmol* **6**, 1325-1333 (2012).

26 Wubben, T. J., Besirli, C. G. & Zacks, D. N. Pharmacotherapies for Retinal Detachment. *Ophthalmology* **123**, 1553-1562(2016).

27 Assi A, Khoueir Z, Helou C, Fakhoury H & Cherfan G. Intraocular application of Mitomycin C to prevent proliferative vitreoretinopathy in perforating and severe intraocular foreign body injuries. *Eye (Lond)*(2019).

28 Sohn EH, Strohbehn A, Stryjewski T, Brodowska K, Flamme-Wiese MJ, Mullins RF, *et al.* POSTERIORLY INSERTED VITREOUS BASE: Preoperative Characteristics, Intraoperative Findings, and Outcomes After Vitrectomy. *Retina*, (2019).

29 Wang HF, Ma JX, Shang QL, An JB, Chen HT, Wang CX. Safety, pharmacokinetics, and prevention effect of intraocular crocetin in proliferative vitreoretinopathy. *Biomed Pharmacother* **109**, 1211-1220(2019).

30 Asaria RH & Charteris DG. Proliferative vitreoretinopathy: developments in pathogenesis and treatment. *Compr Ophthalmol Update* **7**, 179-185 (2006).

31 Di Lauro S, Kadhim MR, Charteris DG & Pastor JC. Classifications for Proliferative Vitreoretinopathy (PVR): An Analysis of Their Use in Publications over the Last 15 Years. *J Ophthalmol* **2016**, 7807596 (2016).

32 Wong CA, Potter MJ, Cui JZ, Chang TS, Ma P, Maberley AL, *et al.* Induction of proliferative vitreoretinopathy by a unique line of human retinal pigment epithelial cells. *Can J Ophthalmol* **37**, 211-220 (2002).

33 Kulasinghe A, Taheri T, O'Byrne K, Hughes BGM, Kenny L, Punyadeera C. Highly Multiplexed Digital Spatial Profiling of the Tumor Microenvironment of Head and Neck Squamous Cell Carcinoma Patients. *Front Oncol* **10**, 607349 (2020).

34 Krassowski M, Das V, Sahu SK & Misra BB. State of the Field in Multi-Omics Research: From Computational Needs to Data Mining and Sharing. *Front Genet* **11**, 610798(2020).

35 Lei H, Velez G, Cui J, Samad A, Maberley D, Matsubara J, *et al.* N-Acetylcysteine Suppresses Retinal Detachment in an Experimental Model of Proliferative Vitreoretinopathy. *Am J Pathol* **177**, 132-140 (2010).

36 Ma G, Duan Y, Huang X, Qian CX, Chee Y, Mukai S, *et al.* Prevention of Proliferative Vitreoretinopathy by Suppression of Phosphatidylinositol 5-Phosphate 4-Kinases. *Invest Ophthalmol Vis Sci* **57**, 3935-3943 (2016).

37 Anzalone AV, R. P., Davis JR, Sousa AA, Koblan LW, Levy JM, Chen PJ,

Wilson C, Newby GA, Raguram A, Liu DR. Search-and-replace genome editing without double-strand breaks or donor DNA. *Nature* **576**, 149-157 (2019).

38 Lei, H. & Kazlauskas, A. Growth factors outside of the PDGF family employ ROS/SFKs to activate PDGF receptor alpha and thereby promote proliferation and survival of cells. *J Biol Chem.* **284**, 6329-6336 (2009).

39 Lei H, Qian CX, Lei J, Haddock LJ, Mukai S, *et al.* RasGAP Promotes Autophagy and Thereby Suppresses Platelet-Derived Growth Factor Receptor-Mediated Signaling Events, Cellular Responses, and Pathology. *Mol Cell Biol* **35**, 1673-1685 (2015).

40 Liu B, Song J, Han H, Hu Z, Chen N, Cui J, et al. Blockade of MDM2 with inactive Cas9 prevents epithelial to mesenchymal transition in retinal pigment epithelial cells. *Lab Invest* **99**, 1874-1886 (2019).

41 Lei H, Velez G, Hovland P, Hirose T, Gilbertson D, Kazlauskas A. Growth factors outside the PDGF family drive experimental PVR. *Invest Ophthalmol Vis Sci* **50**, 3394-3403 (2009).

42 Lei H, Rheaume MA, Cui J, Mukai S, Maberley D, Samad A, *et al.* A novel function of p53: a gatekeeper of retinal detachment. *Am J Pathol* **181**, 866-874 (2012).

43 Fastenberg, D. M., Diddie, K. R., Sorgente, N. & Ryan, S. J. A comparison of different cellular inocula in an experimental model of massive periretinal proliferation. *Am J Ophthalmol* **93**, 559-564 (1982).

44 Huang X, Zhou G, Wu W, Duan Y, Ma G, Song J, *et al.* Genome editing abrogates angiogenesis in vivo. *Nature communications* **8**, 112 (2017).

45 Shukal D, Bhadresha K, Shastri B, Mehta D, Vasavada A, Johar K, *et al.* Dichloroacetate prevents TGFbeta-induced epithelial-mesenchymal transition of retinal pigment epithelial cells. *Exp Eye Res* **197**, 108072 (2020).

46 Yao H, Ge T, Zhang Y, Li M, Yang S, Li H, *et al.* BMP7 antagonizes proliferative vitreoretinopathy through retinal pigment epithelial fibrosis in vivo and in vitro. *FASEB journal* **33**, 3212-3224 (2019).

47 Connor TB, Roberts AB, Sporn MB, Danielpour D, Dart LL, Michels RG, *et al.* Correlation of fibrosis and transforming growth factor-beta type 2 levels in the eye. *J Clin Invest* **83**, 1661-1666 (1989).

48 Han H, Zhao X, Liao M, Song Y, You C, Dong X, *et al.* Activated Blood Coagulation Factor X (FXa) Contributes to the Development of Traumatic PVR Through Promoting RPE Epithelial-Mesenchymal Transition. *Invest Ophthalmol Vis Sci* **62**, 29 (2021).

49 Miller CG, Henderson M, Mantopoulos D, Leskov I, Greco T, Schwarzbauer JE, *et al.* The Proteome of Preretinal Tissue in Proliferative Vitreoretinopathy. *Ophthalmic Surg Lasers Imaging Retina* **52**, S5-S12(2021).

50 Agrawal RN, He S, Spee C, Cui JZ, Ryan SJ, Hinton DR. *et al.* In vivo models of proliferative vitreoretinopathy. *Nat Protoc* **2**, 67-77(2007).

51 Wu W, Zhou G, Han H, Huang X, Jiang H, Mukai S, *et al.* PI3Kdelta as a Novel Therapeutic Target in Pathological Angiogenesis. *Diabetes* **69**, 736-748

(2020).

52 Immonen I, Tervo K, Virtanen I, Laatikainen L & Tervo T. Immunohistochemical demonstration of cellular fibronectin and tenascin in human epiretinal membranes. *Acta Ophthalmol (Copenh)* **69**, 466-471(1991).

53 Grisanti S, Heimann, K. & Wiedemann, P. Origin of fibronectin in epiretinal membranes of proliferative vitreoretinopathy and proliferative diabetic retinopathy. *Br J Ophthalmol* **77**, 238-242 (1993).

54 Altera A, Tosi GM, Regoli M, De Benedetto E & Bertelli E. The extracellular matrix complexity of idiopathic epiretinal membranes and the bilaminar arrangement of the associated internal limiting membrane in the posterior retina. *Graefes Arch Clin Exp Ophthalmol* **259**, 2559-2571(2021).

55 Hou H, Nudleman E & Weinreb RN. Animal Models of Proliferative Vitreoretinopathy and Their Use in Pharmaceutical Investigations. *Ophthalmic Res*, 1-10 (2018).

56 Lei H, Hovland P, Velez G, Haran A, Gilbertson D, Hirose T, *et al.* A potential role for PDGF-C in experimental and clinical proliferative vitreoretinopathy. *Invest Ophthalmol Vis Sci* **48**, 2335-2342 (2007).

57 Peyman GA & Schulman J. Proliferative vitreoretinopathy and chemotherapeutic agents. *Surv Ophthalmol* **29**, 434-442(1985).

58 Sadaka A, Sisk RA, Osher JM, Toygar O, Duncan MK, Riemann CD. Intravitreal methotrexate infusion for proliferative vitreoretinopathy. *Clin Ophthalmol* **10**, 1811-1817 (2016).

59 Umazume K, Liu L, Scott PA, de Castro JP, McDonald K, Kaplan HJ, *et al.* Inhibition of PVR with a tyrosine kinase inhibitor, dasatinib, in the swine. *Invest Ophthalmol Vis Sci* **54**, 1150-1159 (2013).

60 Imai K, Loewenstein A, Koroma B, Grebe R & de Juan E. Herbimycin A in the treatment of experimental proliferative vitreoretinopathy: toxicity and efficacy study. *Graefes Arch Clin Exp Ophthalmol* **238**, 440-447 (2000).

61 Nassar K, Grisanti S, Tura A, Luke J, Luke M, Soliman M, *et al.* A TGF-beta receptor 1 inhibitor for prevention of proliferative vitreoretinopathy. *Exp Eye Res* **123**, 72-86 (2014).

62 Idrees S, Sridhar J & Kuriyan AE. Proliferative Vitreoretinopathy: A Review. *Int Ophthalmol Clin* **59**, 221-240 (2019).

Ethics Approval/Consent to Participate

Ethical approvals for harvesting ERMs from patients with PVR at Shenzhen Eye Hospital and for collecting control breast epithelial tissues from patients with breast cancers at Zhejiang Cancer Hospital were obtained from the Ethical Committees of Shenzhen Eye Hospital, Shenzhen, China and at Zhejiang Tumor Hospital, Hangzhou, China, respectively. Patients with PVR or cancer were consent to participate in these research programs, which adhered to the tenets of the Declaration of Hlesinki.

Author Contribution Statement

DL, HH and XH performed the experiments, analyzed the results, and made equal contributions to this work; DF, HQ, ZH, LW, and GM performed some of the

experiments; GZ, JT and BV revised the manuscript; SZ and HL conceived the experiments, analyzed the data and wrote the manuscript.

Funding Statement

This work was supported by the National Natural Science Foundation of China (82070989) to HL, China Scholarship Council (201806320148) to HH, the National Natural Science Foundation of China (81860172) to XH and the Sanming Project of Medicine in Shenzhen (SZSM202011015) to GZ, SZ and HL. No funding bodies had any role in the study design, data collection and analysis, decision to publish or preparation of the manuscript.

Data Availability Statement

The materials described in this report, including all relevant raw data, will be freely available to any researcher wishing to use them for noncommercial purposes, without breaching participant confidentiality. I

Conflicts of interest

B.V. is a consultant for Karus Therapeutics (Oxford, UK), iOnctura (Geneva, Switzerland) and Venthera (Palo Alto, CA, USA) and has received speaker fees from Gilead Sciences (Foster City, US), and all other authors in this article declare that they have no conflicts of interest with the contents of this article.

Figure legends

Figure 1. GeoMx Digital Spatial Profiling of ERMs from patients with PVR

(A) Corresponding regions of interest (ERM: epiretinal membranes from patients with PVR, Control: breast epithelial tissue as a control) were captured for DSP analysis based on immunofluorescent staining for CK (pan-keratin, Green), CD45 (Red) and DAPI (Blue). Scale bar: 500 μm.

(B, C) Volcano Plot : The X-axis of the figure is the protein difference multiple (take log2), and the Y-axis is the corresponding -log10 (P value). In the figure, the red points are significantly up-regulated proteins, the green points are significantly down-regulated proteins, and the gray points are proteins that have no significant changes. **(B)** Control tissue *versus* PVR membrane; **(C)** Epithelial cells *versus* immune cells in the ERMs from patients with PVR. SMA: smooth muscle actin, CK: pan cytokeratin, CTLA-4 (cytotoxic T-lymphocyte-associated protein 4 or CD152) and PD-L1 (programmed death-ligand 1).

(D, E) Assessment of IgG as normalizers. Clustered heatmap of relative expression of proteins per ROI. Ward D2 clustering was applied, followed by K-means clustering to delineate differences between expression profiles among compartments. CTL: control (normal tissue); ERM: PVR membranes. D: CD68, Fibronectin, S6, SMA, PD-L1, C56, CD11c, HLA-DR, CTLA4, CD45, CD4, CD6, GZMB, Histone H3, PanCK, RbIG, Mslog2a, Ki-67, beta-2-microglobulin, PD-1, CD20, CD3, Ms IgG1, GADPH; E: SMA, GADPH, Fibronectin, PanCK, CD56, CD8, Histon H3, PD-1, S6, Rb IgG, CD45, CTLA4, CD11c, MsIg2a, CD3, PD-L1, beta-2-microglobulin, CD4, GZMB,

CD20, Ki67, CD68, HLA-DR, MsIgG1; E:

(F, G) Principal Component Analysis (PCA). The X-axis is the first principal component and the Y-axis is the second principal component.

Figure 2. Idelalisib inhibited Akt activation induced by TGF-β2 in human RPE cells

(A) Serum-starved ARPE-19 cells were treated with TGF-β2 (10 ng/ml) or in addition to idelalisib (10 μM) for 24 h and 48 h. Their lysates were subjected to western blotting analysis using indicated antibodies. Shown is a representative of at least three independent experiments.

(B) The bar graphs are mean ± SD of three independent experiments. The data of the intensity of bands was analyzed using one-way ANOVA followed by the Tukey HSD post hoc-test. ***$P < 0.001$.

Figure 3. Idelalisib blocked TGF-β2 induced collagen gel contraction

RPEM cells were re-suspended in 1.5 mg/ml of neutralized collagen I (pH 7.2) at a density of 1 x10^6 cells/ml and seeded into wells of a 24-well plate that had been pre-incubated overnight with 5 mg/ml (BSA/PBS). The collagen was solidified by incubation at 37°C for 90 minutes. The polymerized gels were overlaid with DMEM/F12 alone (-) or TGF-β2 (10 ng/ml) supplemented with idelalisib (10 μM) or its vehicle as indicated. 48 hours later, the gel diameter was measured and the gel area calculated using the formula: $3.14 \times r^2$. The bar graphs represent the mean ± SD of the three independent experiments; *** denotes $p < 0.001$ using one-way ANOVA followed by the Tukey HSD post hoc-test. A photograph of the representative

experiment in A is shown at the bottom of the bar graphs.

Figure 4. Examination of idelalisib toxicity in rabbit eyes

Idelalisib was injected into the rabbit vitreous to achieve a final vitreal concentration of 10 or 20 μM (2 rabbits per dose). This day was considered day 0. The rabbits underwent fundus examinations by experienced ophthalmologists on days 1, 3, 5, and 7. On day 7, the rabbit eyes were examined by electroretinogram (ERG, dark adaption) (**A**) and optical coherence tomography (OCT) (**B**). Subsequently, the eyeballs from the euthanized rabbits were subjected to histological analysis by hematoxylin & eosin stain (**C**). Arrows in B point to retinas. Representative data are presented in each panel for the indicated concentration. Scale bar: 200 μm.

Figure 5. Idelalisib prevented experimental PVR in rabbits

PVR was induced in the right eyes of 8-weeks-old Dutch Belted pigmented rabbits. Briefly, one week after gas vitrectomy, rabbits were injected intravitreally with platelet-rich plasma (PRP, 0.1 ml) and RPEM cells (3.0 x 10^5 cells) supplemented with either idelalisib (10 μM, **9** rabbits) or its vehicle (0.01% DMSO, **8** rabbits).

(**A**) The eyes of the rabbits were examined at the indicated times by two masked ophthalmologists using a double blind approach, and the PVR status for each rabbit was plotted. Each symbol denotes a rabbit injected intravitreally with drug vehicle (triangle, 8 rabbits in total) and idelalisib (solid circle, 9 rabbits). The numbers in the Y-Axis denote PVR stages (0 -5). PVR stage 0: the eye is normal; stage 1: there were some fibrosis in the vitreous and intravitreal membranes formation in the eye; stage 2: there were more fibrosis in the vitreous and more intravitreal membranes than those in the stage 1, and there were focal traction and localized ocular changes, hyperemia,

engorgement and dilation; stage 3: the intravitreal membrane caused localized detachment of retinal and medullary ray; stage 4: there were extensive retinal detachment (total medullary ray detachment and peripapillary retinal detachment); stage 5: the retina got total detached from its original position and there were retinal folds and holes. The days in the X-Axis indicate the observation time starting from the day 1 after the intravitreal cell injection. Statistical significance was assessed by Mann-Whitney analysis.

A subset of rabbits was examined on day 28 by (**B**) ERG (4 rabbits): L stands for left eyes without injection and R stands for right eyes injected with idelalisib or its vehicle; (**C**) OCT (6 rabbits): PVR stage 0 (2 rabbits): without fibrosis; stage 2 (1 rabbit): a fibrotic band attached retina (double arrows); stage 3 (1 rabbit): fibrotic bands attached retina and drew the retinal detachment; stage 5 (2 rabbits): the retina got total detached. A single arrow points to the retina and double arrows point to cellular membranes; (**D**) histology (6 eyeballs). The rabbit eyeballs were from stage 0 (2 eyeballs), stage 2 (1 eyeball), stage 3 (1 eyeball) and stage 5 (2 eyeballs). The histological eyeball sections were stained with hematoxylin and eosin; arrowhead and double arrows point to cellular membranes.

Figures

Figure 1

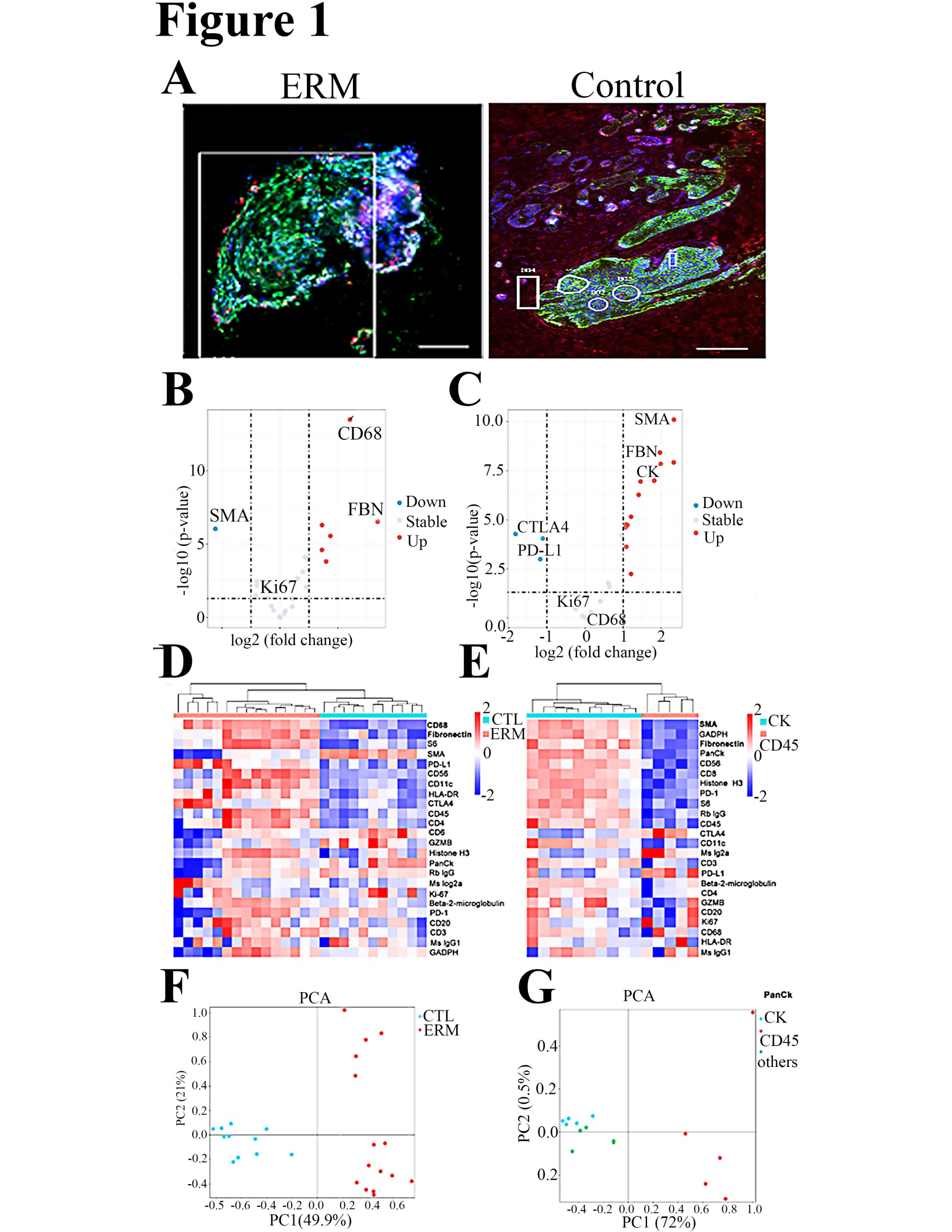
A
ERM
Control
B
CD68
SMA
FBN
Ki67
Down
Stable
Up
-log10 (p-value)
log2 (fold change)
C
SMA
FBN
CK
CTLA4
PD-L1
Ki67
CD68
Down
Stable
Up
-log10(p-value)
log2 (fold change)
D
CTL
ERM
CD68
Fibronectin
S6
SMA
PD-L1
CD56
CD11c
HLA-DR
CTLA4
CD45
CD4
CD8
GZMB
Histone H3
PanCk
Rb IgG
Ms Ig2a
KI-67
Beta-2-microglobulin
PD-1
CD20
CD3
Ms IgG1
GADPH
E
CK
CD45
SMA
GADPH
Fibronectin
PanCk
CD56
CD8
Histone H3
PD-1
S6
Rb IgG
CD45
CTLA4
CD11c
Ms Ig2a
CD3
PD-L1
Beta-2-microglobulin
CD4
GZMB
CD20
Ki67
CD68
HLA-DR
Ms IgG1
F
PCA
CTL
ERM
PC2 (21%)
PC1(49.9%)
G
PCA
PanCk
CK
CD45
others
PC2 (0.5%)
PC1 (72%)

Figure 2

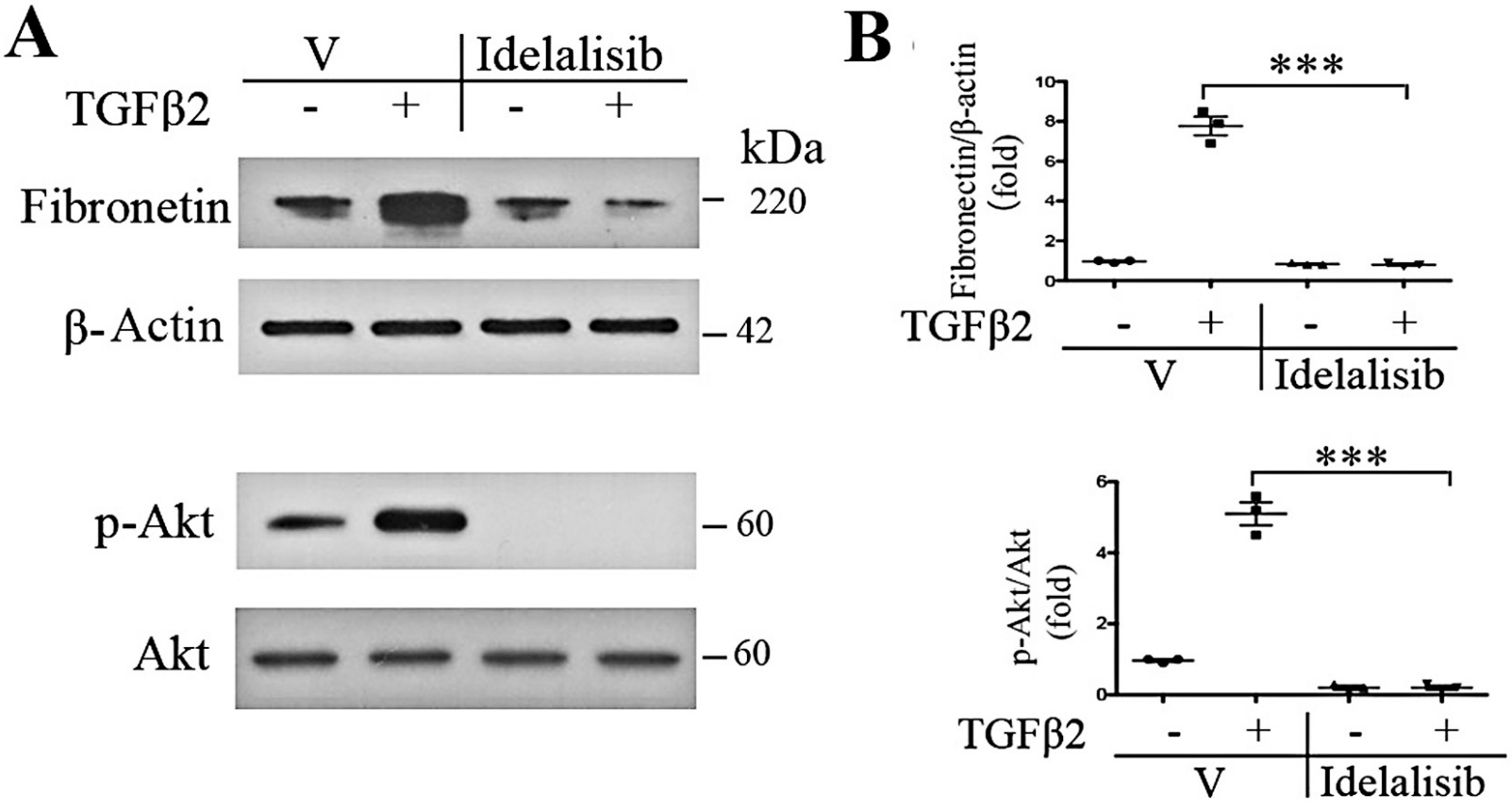
A
V
Idelalisib
TGFβ2
- + - +
kDa
Fibronetin
220
β-Actin
42
p-Akt
60
Akt
60
B
Fibronectin/β-actin (fold)
***
TGFβ2
- + - +
V
Idelalisib
p-Akt/Akt (fold)
***
TGFβ2
- + - +
V
Idelalisib

Figure 3

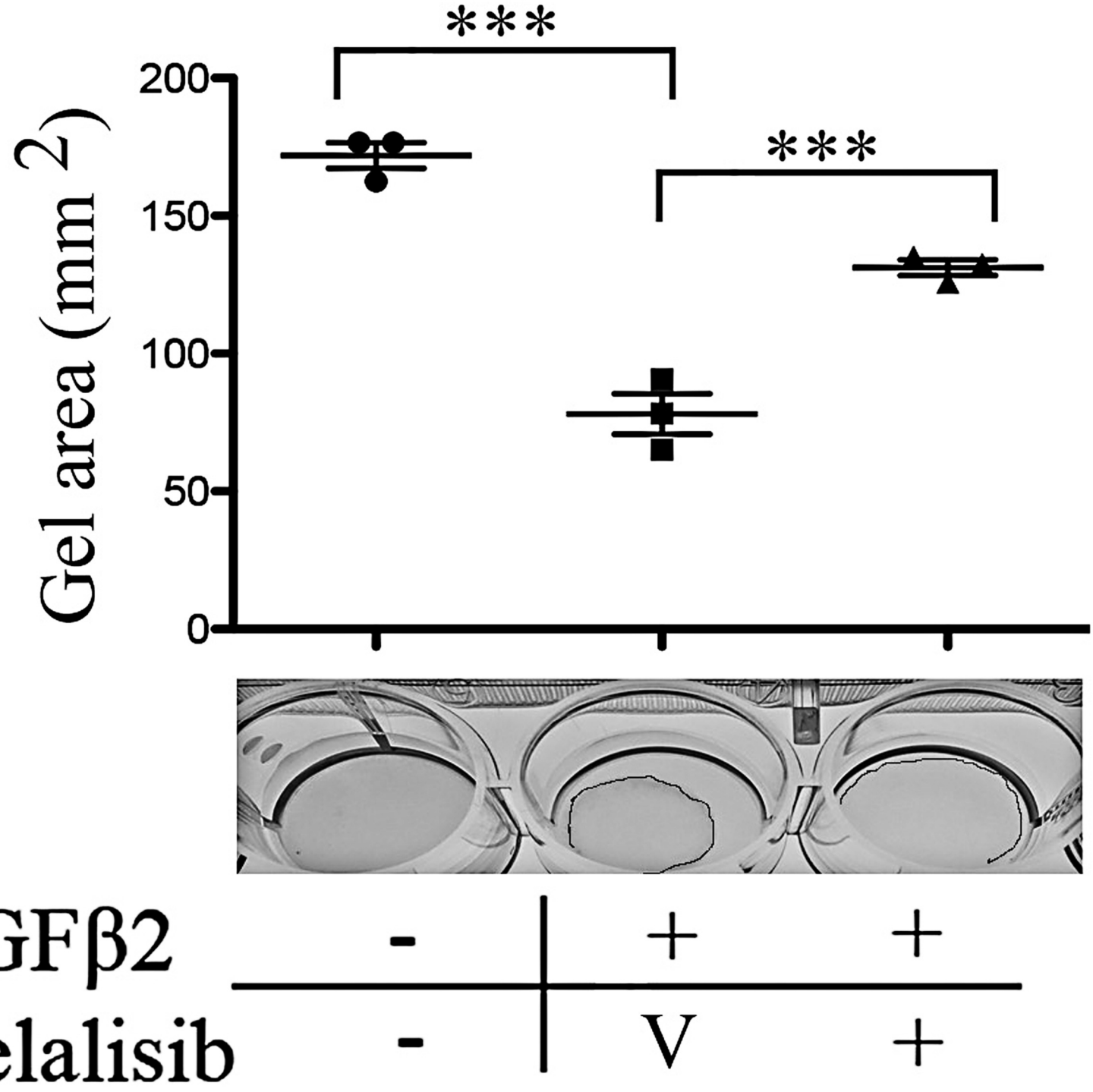

Figure 4

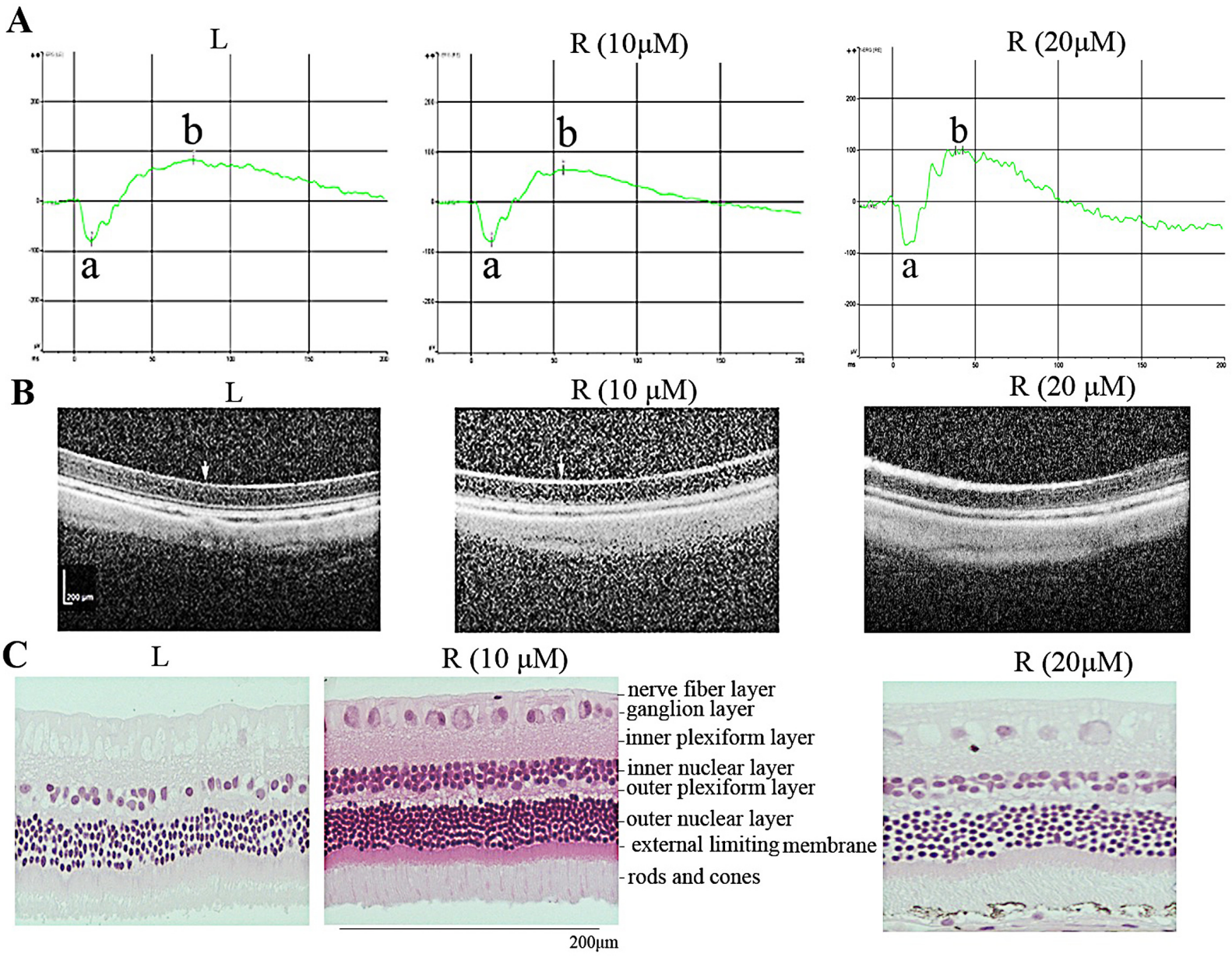
A
L
R (10μM)
R (20μM)
b
a
B
L
R (10 μM)
R (20 μM)
200 μm
C
L
R (10 μM)
R (20μM)
nerve fiber layer
ganglion layer
inner plexiform layer
inner nuclear layer
outer plexiform layer
outer nuclear layer
external limiting membrane
rods and cones
200μm

Figure 5

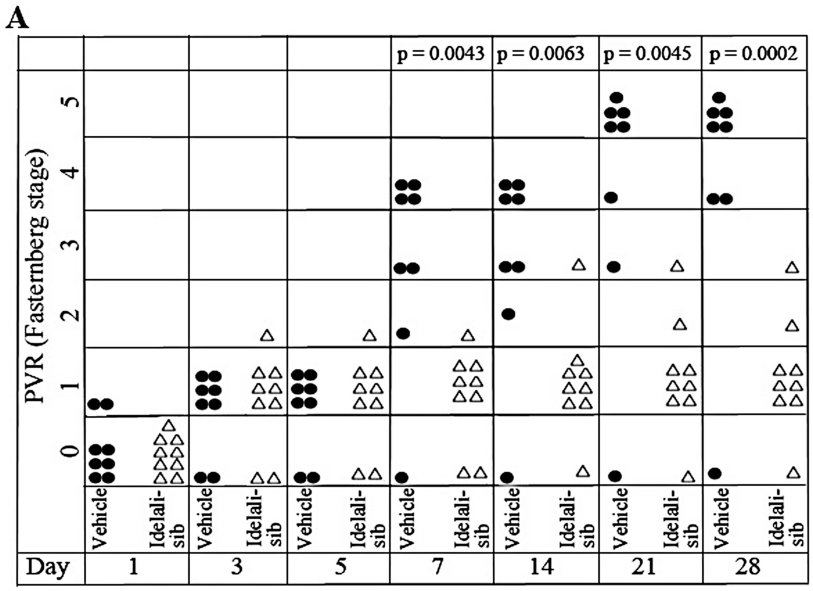
A
p = 0.0043
p = 0.0063
p = 0.0045
p = 0.0002
PVR (Fasternberg stage)
0
1
2
3
4
5
Vehicle
Idelali-sib
Day
1
3
5
7
14
21
28

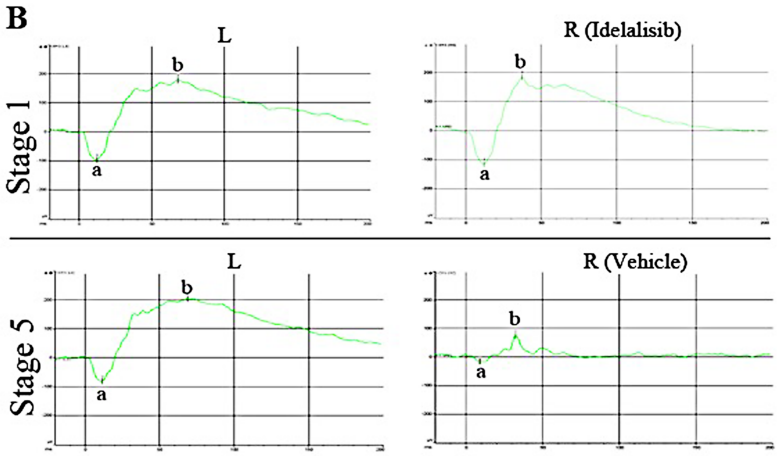
B
L
R (Idelalisib)
Stage 1
a
b
L
R (Vehicle)
Stage 5
a
b

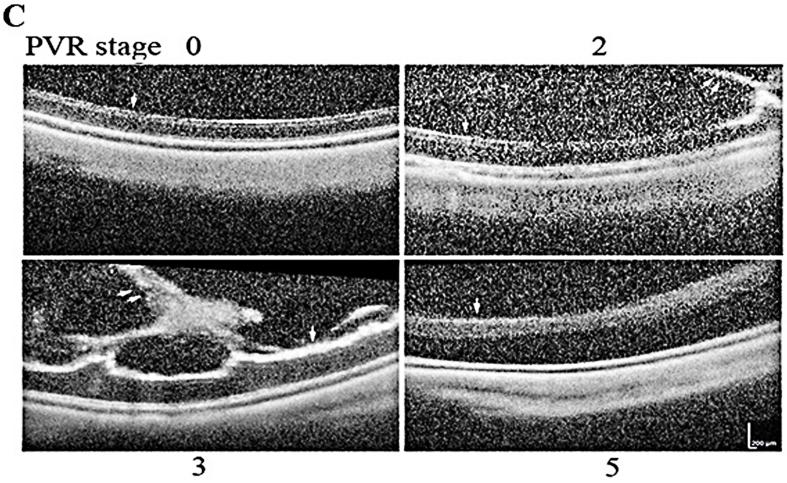
C
PVR stage 0
2
3
5

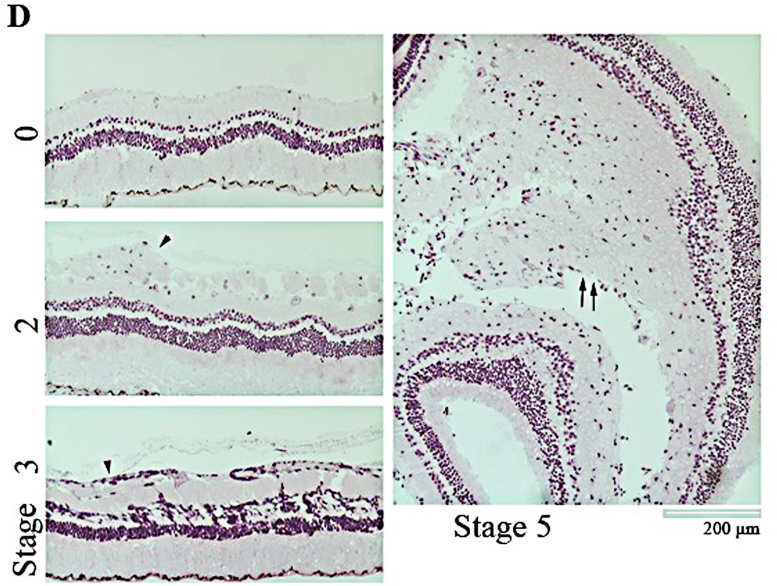
D
0
2
3
Stage
Stage 5
200 µm